JACS
JOURNAL OF THE AMERICAN CHEMICAL SOCIETY
Communication
pubs.acs.org/JACS

Peptide Nanofibers with Dynamic Instability through Nonequilibrium Biocatalytic Assembly

Sisir Debnath, Sangita Roy, and Rein V. Ulijn*

WestCHEM, Department of Pure and Applied Chemistry, University of Strathclyde, 295 Cathedral Street, Glasgow G1 1XL, U.K.

Supporting Information

ABSTRACT: We demonstrate the formation of supramolecular peptide nanofibers that display dynamic instability; i.e., they are formed by competing assembly and disassembly reactions, where assembly is favored *away* from equilibrium. The systems are based on competitive catalytic transacylation and hydrolysis, producing a self-assembling aromatic peptide amphiphile from amino acid precursors that temporarily exceeds the critical gelation concentration, until the competing hydrolytic reaction takes over. Analysis by atomic force microscopy shows consecutive nanofiber formation and shortening. The process results in macroscopically observable temporary hydrogelation, which may be repeated upon refueling the system with further addition of the chemically activated amino acid precursor. Nonequilibrium nanostructures open up opportunities for mimicry of the behavior of dynamic gels found in natural systems and provide components for future adaptive nanotechnologies.

The combination of molecular self-assembly[1] and (bio)-catalysis underlies dynamic processes in biology and also provides a useful paradigm for fabrication of adaptive nanostructures.[2] A key feature of naturally occurring catalytic self-assembling systems is that they are dynamic in nature, with lengthening and breakdown tightly regulated. For example, catalytic formation and degradation of actin filaments[3] and microtubules[4] underlie vital cellular functions such as motility, differentiation, and division. Synthetic mimics of these systems have been the focus of considerable research efforts in recent years.[1,2] One way most man-made systems differ from their natural counterparts is that the latter (e.g., microtubules) display dynamic instability, in that they are assembled and lengthened in a process that relies on energy input (*away* from equilibrium) and shortened when equilibrium is approached. Significant effort is currently invested in developing non-equilibrium molecular systems[5] and materials which may give rise to new features that are normally not associated with synthetic systems, in that they may be reconfigurable, externally fuelled, self-healing, or even self-replicating.[6]

Boekhoven et al. recently published a first example of a nonequilibrium catalytic self-assembly system demonstrating temporary hydrogelation based on catalytic esterification of a diacid.[7] Von Maltzahn et al. demonstrated a nonequilibrium biocatalytic nanoparticle assembly system which could assemble upon kinase/adenosine triphosphate (ATP)-driven phosphorylation and subsequently disassemble in response to a phosphatase enzyme.[8] ATP-driven biocatalytic assembly/disassembly of supramolecular fibers has also been demonstrated using phosphatase/kinase systems.[9] However, for these systems the ATP-driven reaction results in formation of the phosphorylated, nonassembling species, and these are therefore not examples of dynamic instability or nonequilibrium self-assembly.

Thus, we set out to produce nonequilibrium biocatalytic self-assembled systems displaying dynamic instability. The requirements for such a system are the following: (i) the product of the forward reaction should have a tendency for unidirectional self-assembly; (ii) forward and backward reactions to produce/degrade gelator molecules should follow distinct routes; (iii) conditions must be chosen where the critical assembly concentration to form nanofibers is higher than the equilibrium yield of the enzymatic peptide synthesis reaction.

In order to satisfy criterion (i), our system is based on naphthalene-dipeptide gelators where the N-terminus is functionalized with an aromatic group, naphthoxyacetyl (Nap).[10] We used Nap-dipeptide molecules which have the ability to assemble into unidirectional nanofibers through a combination of π-stacking interactions between the aromatic groups and hydrogen-bonding interactions between the peptide backbones, ultimately forming a self-supporting hydrogel.[10] We recently demonstrated that enzymatic condensation of suitable pairs of naphthalene-amino acid with hydrophobic amino acid amides gives Nap-peptide-NH_2, which are highly efficient in hydrogelation.[10c]

Proteases are known to catalyze the synthesis (rather than hydrolysis) of peptides under appropriate conditions.[11] This has been demonstrated, e.g., in organic media, at solid/liquid interfaces, or in highly concentrated heterogeneous systems. We previously demonstrated that molecular self-assembly may also provide a suitable thermodynamic driving force, where the relative stabilization of the peptide product through self-assembly provides a driving force to favor peptide synthesis.[12]

α-Chymotrypsin is well known for its ability to catalyze peptide synthesis starting from a suitable ester precursor to kinetically overcome the bias for hydrolysis in aqueous systems.[11] Qin et al. recently employed this enzyme for biocatalytic self-assembly by using dipeptide esters instead of free acids to form polypeptides that resulted in stable self-assembling structures, produced via transacylation using α-chymotrypsin and papain.[13] Based on this work and in order to meet criterion (ii), we used α-chymotrypsin-catalyzed trans-

Received: August 20, 2013
Published: October 22, 2013

   dx.doi.org/10.1021/ja4086353 | J. Am. Chem. Soc. 2013, 135, 16789−16792

acylation for the forward reaction (under kinetic control), with the competing disassembly reaction based on amide hydrolysis (under thermodynamic control).

Specifically, we used as the acyl donor tyrosine methyl ester (**1**, Figure 1A) with a series of hydrophobic amino acids,

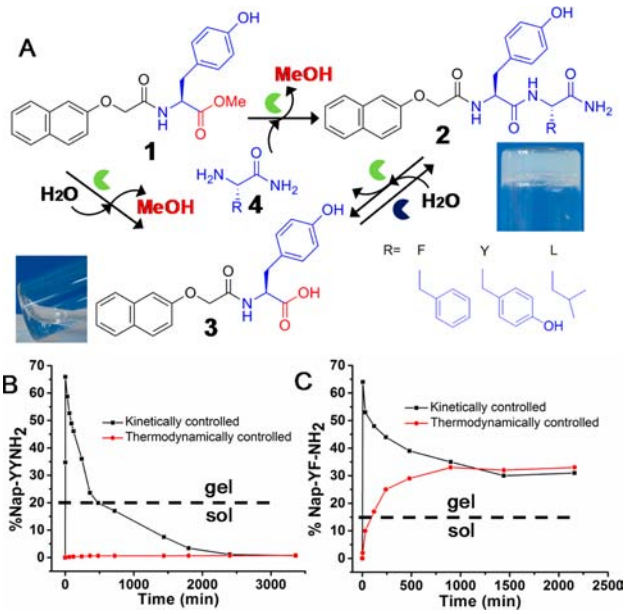

Figure 1. Nonequilibrium biocatalytic self-assembly. (A) Nap-Y-OMe (**1**) and different amino acid amides (X-NH_2, **4**) in the presence of chymotrypsin (green) form the (temporary) hydrogelator (**2**) which may also be hydrolyzed by the same enzyme to Nap-Y-OH (**3**) and **4**. Thermolysin (blue) catalyzes the reversible hydrolysis/condensation of **2**. (B) Nonequilibrium assembly and hydrogelation. Time course of the kinetically controlled reaction (chymotrypsin catalyzed) of Nap-Y-OMe (black line) and thermodynamically controlled reaction (thermolysin catalyzed) of Nap-Y-OH (red line) with Y-NH_2 at pH 8. (C) Reactions of Nap-Y-OMe (black line) and Nap-Y-OH (red line) with F-NH_2 by chymotrypsin and thermolysin, respectively, at pH 8.

functionalized as amides at the C-terminus [L-tyrosine amide (Y-NH_2), L-phenylalanine amide (F-NH_2), L-leucine amide (L-NH_2)], to yield the dipeptide amides (**2**, Figure 1A, Table 1), and reactions were followed using high-performance liquid chromatography (HPLC). Effective transacylation reactions

Table 1. Chymotrypsin-Triggered Self-Assembly and Disassembly of Nap-Y-OMe and Different Amino Acid Amides

entry[a]	X-NH_2	conversion (%) of the dipeptide[b]	time (h)[c]	gelator (%)[d]	CGC (mM)[e]	final conversion (%)[f]
1	YNH_2	69/67[g]	4	20	4	0/0[g]
2	FNH_2	65/64[g]	>40	15	3	14/30[g]
3	LNH_2	57/49[g]	4	23	4.6	0/27[g]

[a]All reactions were performed at 20 mM concentration of both Nap-Y-OMe and X-NH_2 with 1 mg of α-chymotrypsin (lyophilized powder) at pH 10. [b]Conversion reached within 5 min. [c]Lifetime of macroscopically observed gel phase. [d]% of the corresponding gelator during macroscopic transition from gel to sol phase. [e]CGC were estimated by % gelator present during observed gel–sol transition. [f]Final conversions were taken after 40 h. [g]These conversions are obtained at pH 8.

were observed in presence of α-chymotrypsin. The starting material, Nap-Y-OMe (**1**), disappeared within 1 min, and the conversion to the dipeptide product, Nap-YX-NH_2 (**2**), reached a maximum within 2–3 min. The product eventually broke down to the corresponding acid, Nap-Y-OH (**3**), with time. **1** was completely converted through hydrolysis to **3** and acylation to **2**. Over time, amide hydrolysis of **2** to form **3** and **4** started to compete, and the system eventually reached an equilibrium situation. As is shown in Figure 1B,C, there are now two different possible scenarios, resulting in equilibrium or nonequilibrium hydrogelation. Depending on the critical gelation concentration (CGC) of the system, it either reverts back to a solution (equilibrium conversion of **2** < CGC, as observed for Nap-YY-NH_2 and Nap-YL-NH_2 with negligible peptide present at equilibrium; i.e., criterion (iii) is met, nonequilibrium hydrogelation) or remains as a gel (equilibrium conversion of **2** > CGC as observed for Nap-YF-NH_2, giving rise to ~30% final conversion).[14] In either scenario, the final state of the system (hydrogel or solution) is dictated by the self-assembly propensity of the Nap-peptide-NH_2.

To demonstrate that the final conversions indeed represent equilibrium, we used Nap-Y-OH (**3**), the free carboxylic acid, as the acyl donor to couple with F-NH_2 (**4**). The process was catalyzed by chymotrypsin and took 96 h to reach equilibrium (Figure S1). We therefore used thermolysin, an enzyme that was previously shown to be highly efficient in catalyzing direct condensation of free acids and amides,[10c,12] to establish the equilibrium position for Nap-Y-OH with Y-NH_2 or F-NH_2, giving rise to a final yield identical to that observed for the kinetically controlled reaction (Figures 1B,C, S2, and S3). The system remained a solution with negligible conversion for Nap-YY-NH_2 while Nap-YF-NH_2 formed a gel, demonstrating that criterion (iii) is met only for the former system. Table 1 (see also Figures S2–S6) shows the corresponding conversion to the naphthalene dipeptide products and their subsequent hydrolysis.

The lifetime of the gel could be tuned by changing the pH of the solution. Indeed, the dynamic character of the system, i.e., the change in the self-assembly and disassembly, was found to be enhanced at the considerably alkaline pH of 10 (8 h), compared to pH 8 (36 h) (Table 1 and Figure S7). The Nap-YY-NH_2 system at pH 10 was therefore selected for further study.

Figure 2A shows the macroscopic appearance of the reaction mixture over time at pH 10. Analysis by HPLC showed that peptide formation is almost instantaneous (Figure S8). To probe the structural changes at the microscopic level, atomic force microscopy (AFM) was carried out at different time points (Figure 2B–E). Early-stage AFM showed a highly entangled fiber network. These fibers were found to be >10 μm in length (Figure 2B). After 3 h, AFM showed substantial shortening of fibers, 5–6 μm long; however, at this stage the gel remained intact owing to the presence of **2** at a concentration of 35–40%, i.e., above the CGC (Figure 2C). At 5 h, we observed even shorter fibers of length 2–3 μm (Figure 2D), corresponding to a viscous phase with a concentration of Nap-YY-NH_2 ~15%, as evident from the HPLC (Figure S8). On complete hydrolysis of the Nap-dipeptide amide, we observed formation of spherical aggregates, representing Nap-Y-OH, resulting in the formation of the free-flowing solution (Figure 2E). This shortening of fibers provides clear evidence of a dynamically unstable system.

dx.doi.org/10.1021/ja4086353 | J. Am. Chem. Soc. 2013, 135, 16789–16792

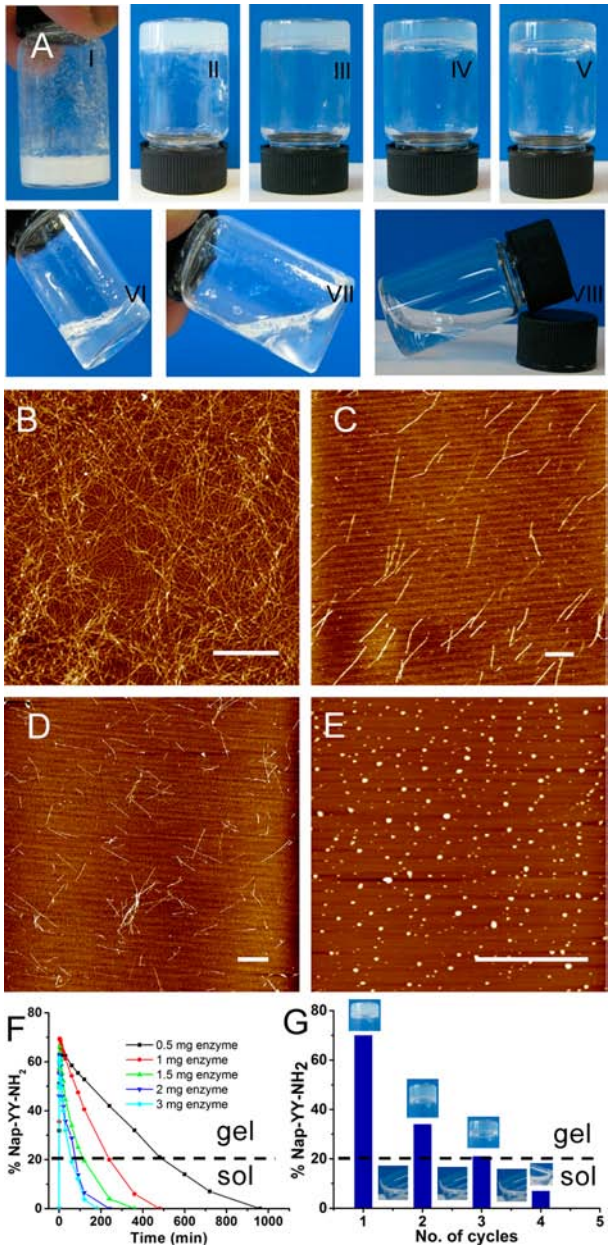

Figure 2. (A) (I–VIII) Photographs of the gel of Nap-YY-NH_2 (prepared with 1 mg of chymotrypsin, pH 10) at 1 min, 5 min, 1 h, 2 h, 3 h, 4 h, 5 h, and 8 h after the reaction. (B–E) AFM images of the morphology of Nap-YY-NH_2 at 30 min, 3 h, 5 h, and 8 h (scale bar, 2 μM). (F) Synthesis and degradation of Nap-YY-NH_2 over the course of time in the presence of 0.5–3 mg of chymotrypsin. (G) Refueling the system with Nap-Y-OMe to form the gel repeatedly.

In order to assess the possibility of tuning the lifetime of the gel, we varied the enzyme concentrations from 0.05 to 3 mg/mL (Figures 2F, S8, and S9). The initial coupling step showed limited dependence on enzyme amount when the concentration of the enzyme is >0.5 mg/mL (Figure 2F). However, the competing reaction, i.e., hydrolysis of the dipeptide amide, was found to be sensitive to the enzyme concentration. At 0.5 mg/mL, complete hydrolysis and gel dissolution occur after 16 h, while with 3 mg/mL enzyme, complete hydrolysis takes place within only 3 h. At lower concentrations of enzyme (0.1 and 0.05 mg/mL), both the initial coupling step and the hydrolysis of the dipeptide depend on the concentration. For 0.1 and 0.05 mg/mL, the maximum conversion was found to be 59% and 52%, respectively, compared to 69% for 1 mg/mL. The hydrolysis step was also found to be much slower: even after 7 days, 9% of the product Nap-YY-NH_2 was detected for 0.05 mg/mL enzyme concentration (Figure S9). These results show that gel lifetime can easily be controlled by changing the concentration of the enzyme. The nanofibers do not have significant inhibitory effects on the enzyme since different densities of fibers gave similar degradation rates (Figure S10).

To investigate the possibility of repeated temporary hydrogelation, we added another equivalent of **1** (after 24 h) and found that, on refueling, gel fibers were formed and eventually broken down again. This process could be repeated up to three cycles, after which the dipeptide conversion could not reach the CGC, thought to be related to accumulation of Nap-Y-OH in the system, since the presence of Nap-Y-OH reduces final yield (Figure S11). In the future, *in situ* reactivation of Nap-Y-OH to Nap-Y-OMe would provide an interesting direction. Attempts to refuel by esterification of Nap-Y-OH to Nap-Y-OMe using methyl iodide, as demonstrated previously by Boekhoven et al.,[7] lacked the selectivity required for the peptide-based system used here, and we are currently seeking biocatalytic routes to achieve *in situ* reactivation.

Insights into supramolecular interactions underpinning the system were obtained through fluorescence and circular dichroism (CD) spectroscopy. π-Stacking interactions between the aromatic groups are known to be the major driving force in the self-assembly of aromatic peptide amphiphiles.[10] These interactions can be monitored using fluorescence spectroscopy, which shows the change in the environment of the naphthalene fluorophore. Fluorescence emission spectra of Nap-YY-NH_2 showed a characteristics peak at 355 nm (Figure S12A). We observed a sharp quenching of the monomeric emission in the initial few minutes owing to the formation of the dipeptide amide and subsequent self-assembly (Figure S12A inset). Red-shifted excimer peaks at higher wavelengths, as observed previously with other aromatic groups,[15] were not observed.

Chirally organized aromatics in the gel state are known to give rise to intense CD signals.[16] Such CD signals arise from the chiral organization of the self-assembling building blocks in the gel state, rather than from the inherent molecular chirality of the chromophores. During the initial few minutes, we observed an extensive CD signal with two maxima at 290 and 335 nm, corresponding to π–π^* and n–π^* transitions of the naphthalene chromophore (Figure S12B).[10a,c] With time the intensity of the CD signal was found to be reduced (Figure S12B inset), owing to the breakdown of the supramolecular assembly of the dipeptide product to the corresponding acid. After 8 h the system was CD silent, which was indicative of complete disassembly of the Nap-YY-NH_2 and formation of micellar Nap-Y-OH.

These structural changes were also reflected in the rheological properties of the self-assembled system. Initially, an increase of the mechanical strength from 2.79 to 2.92 kPa is observed (Figure S14). As soon as the hydrolysis/disassembly initiates, the gel strength is reduced. After 4 h, when the dipeptide concentration reaches around 20%, the strength is found to be only 0.024 kPa, after which the gel dissolves. We then investigated whether the mechanical strength of the resulting hydrogels influences hydrolysis and dissolution. We measured the stiffness of all three gels, Nap-YF-NH_2 giving the highest stiffness (14.3 kPa, Figure S15) compared to the other two (5.8 kPa for Nap-YL-NH_2 and 2.9 kPa for Nap-YY-NH_2,

dx.doi.org/10.1021/ja4086353 | J. Am. Chem. Soc. 2013, 135, 16789–16792

Figures S14 and S16). This observation could explain the corresponding dissolution rate of the peptide nanofibers with Nap-YF-NH_2, taking a longer time to degrade compared to the weaker gelators.

In summary, we developed a nonequilibrium biocatalytic self-assembling system that uses chemical energy stored in a methyl ester precursor to generate a temporary high concentration of the gelator in a kinetically controlled manner. Subsequent hydrolysis of the gelator leads to the formation of nanofibers with dynamic instability. The system could be refueled several times. Such a system mimics the unique features of the natural dynamic self-assembled systems but is much simpler and accessible for future adaptive biomedical and nanotechnological applications.

■ ASSOCIATED CONTENT

Ⓢ Supporting Information

Experimental details and characterization data. This material is available free of charge via the Internet at http://pubs.acs.org.

■ AUTHOR INFORMATION

Corresponding Author

rein.ulijn@strath.ac.uk

Notes

The authors declare no competing financial interest.

■ ACKNOWLEDGMENTS

We thank the EPSRC, HFSP, ERC (Starting Grant EMERgE), and Leverhulme Trust (Leadership Award) (U.K.) for funding. The material is based on research sponsored by the Air Force Laboratory, under Agreement FA9550-11-1-0263.

■ REFERENCES

(1) (a) Lehn, J. -M. *Science* **2002**, *295*, 2400−2403. (b) Whitesides, G. M.; Grzybowski, B. *Science* **2002**, *295*, 2418−2421. (c) Aida, T.; Meijer, E. W.; Stupp, S. I. *Science* **2012**, *335*, 813−817.

(2) (a) Wilner, O. I.; Weizmann, Y.; Gill, R.; Lioubashevski, O.; Freeman, R.; Willner, I. *Nat. Nanotechnol.* **2009**, *4*, 249−254. (b) Ostrov, N.; Gazit, E. *Angew. Chem., Int. Ed.* **2010**, *49*, 3018−3021. (c) Hirst, A. R.; Roy, S.; Arora, M.; Das, A. K.; Hodson, N.; Murray, P.; Marshall, S.; Javid, N.; Sefcik, J.; Boekhoven, J.; van Esch, J. H.; Santabarbara, S.; Hunt, N. T.; Ulijn, R. V. *Nature Chem.* **2010**, *2*, 1089−1094. (d) Ku, T.-H.; Chien, M.-P.; Thompson, M. P.; Sinkovits, R. S.; Olson, N. H.; Baker, T. S.; Gianneschi, N. C. *J. Am. Chem. Soc.* **2011**, *133*, 8392−8395. (e) Li, X.; Kuang, Y.; Lin, H. -C.; Gao, Y.; Shi, j.; Xu, B. *Angew. Chem., Int. Ed.* **2011**, *50*, 9365−9369. (f) Hu, J.; Zhang, G.; Liu, S. *Chem. Soc. Rev.* **2012**, *41*, 5933−5949. (g) Guo, D. -S.; Wang, K.; Wang, Y. -X.; Liu, Y. *J. Am. Chem. Soc.* **2012**, *134*, 10244−10250. (h) Jiang, L.; Yan, Y.; Drechsler, M.; Huang, J. *Chem. Commun.* **2012**, *48*, 7347−7349. (i) Lock, L. L.; Cheetham, A. G.; Zhang, P.; Cui, H. *ACS Nano* **2013**, *7*, 4924−4932. (j) Boekhoven, J.; Poolman, J. M.; Maity, C.; Li, F.; van der Mee, L.; Minkenberg, C. B.; Mendes, E.; van Esch, J. H.; Eelkema, R. *Nature Chem.* **2013**, *5*, 433−437.

(3) Alberts, B.; Johnson, A.; Lewis, J.; Raff, M.; Roberts, K.; Walter, P. *The cytoskeleton. Molecular biology of the cell*; Garland Science: New York, 2002; Chapter 16, pp 907−982.

(4) Desai, A.; Mitchison, T. J. *Annu. Rev. Cell. Dev. Biol.* **1997**, *13*, 83−117.

(5) (a) Warren, S. C.; Guney-Altay, O.; Grzybowski, B. A. *J. Phys. Chem. Lett.* **2012**, *3*, 2103−2111. (b) Mann, S. *Nat. Mater.* **2009**, *8*, 781−792.

(6) (a) Miras, H. N.; Sorus, M.; Hawkett, J.; Sells, D. O.; McInnes, E. J. L.; Cronin, L. *J. Am. Chem. Soc.* **2012**, *134*, 6980−6983. (b) Carnall, J. M. A.; Waudby, C. A.; Belenguer, A. M.; Stuart, M. C. A.; Peyralans, J. J.-P.; Otto, S. *Science* **2010**, *327*, 1502−1506. (c) Rubinov, B.; Wagner, N.; Matmor, M.; Regev, O.; Ashkenasy, N.; Ashkenasy, G. *ACS Nano* **2012**, *6*, 7893−7901.

(7) Boekhoven, J.; Brizard, A. M.; Kowlgi, K. N. K.; Koper, G. J. M.; Eelkema, K.; van Esch, J. H. *Angew. Chem., Int. Ed.* **2010**, *49*, 4825−4828.

(8) von Maltzahn, G.; Min, D.-H.; Zhang, Y. J..; Park, -H.; Harris, T. J.; Sailor, M.; Bhatia, S. N. *Adv. Mater.* **2007**, *19*, 3579−3583.

(9) (a) Winkler, S.; Wilson, D.; Kaplan, D. L. *Biochemistry* **2000**, *39*, 12739−12746. (b) Yang, Z.; Liang, G.; Wang, L.; Xu, B. *J. Am. Chem. Soc.* **2006**, *128*, 3038−3043. (c) Webber, M. J.; Newcomb, C. J.; Bitton, R.; Stupp, S. I. *Soft Matter* **2011**, *7*, 9665−9672.

(10) (a) Yang, Z.; Liang, G.; Ma, M.; Gao, Y.; Xu, B. *J. Mater. Chem.* **2007**, *17*, 850−854. (b) Chen, L.; Morris, K.; Laybourn, A.; Elias, D.; Hicks, M. R.; Rodger, A.; Serpell, L.; Adams, D. J. *Langmuir* **2010**, *26*, 5232−5242. (c) Nalluri, S. K. M.; Ulijn, R. V. *Chem. Sci.* **2013**, *4*, 3699−3705.

(11) (a) Fastrez, J.; Fersht, A. R. *Biochemistry* **1973**, *12*, 2025−2034. (b) Morihara, K.; Oka, T. *Biochem. J.* **1977**, *163*, 531−542. (c) Bordusa, F. *Chem. Rev.* **2002**, *102*, 4817−4867.

(12) (a) Toledano, S.; Williams, R. J.; Jayawarna, V.; Ulijn, R. V. *J. Am. Chem. Soc.* **2006**, *128*, 1070−1071. (b) Williams, R. J.; Smith, A. M.; Collins, R.; Hodson, N.; Das, A. K.; Ulijn, R. V. *Nat. Nanotechnol.* **2009**, *4*, 19−24.

(13) Qin, X.; Xie, W.; Tian, S.; Cai, J.; Yuan, H.; Yu, Z.; Butterfoss, G. L.; Khuonga, A. C.; Gross, R. A. *Chem. Commun.* **2013**, *49*, 4839−4841.

(14) In our previous paper, yields obtained through thermolysin-catalyzed condensation were slightly higher due to the use of a 1:4 molar ratio of Nap-Y and F/L/Y-NH_2.

(15) (a) Gao, J.; Wang, H.; Wang, L.; Wang, J.; Kong, D.; Yang, Z. *J. Am. Chem. Soc.* **2009**, *131*, 11286−11287. (b) Channon, K. J.; Devlin, G. L.; Magennis, S. W.; Finlayson, C. E.; Tickler, A. K.; Silva, C.; MacPhee, C. E. *J. Am. Chem. Soc.* **2008**, *130*, 5487−5491.

(16) (a) Saha, A.; Manna, S.; Nandi, A. K. *Langmuir* **2007**, *23*, 13126−13135. (b) Kimura, M.; Kitamura, T.; Sano, M.; Muto, T.; Hanabusa, K.; Shiraia, H.; Kobayashi, N. *New J. Chem.* **2000**, *24*, 113−114.